VUV photon-induced ionization/dissociation of antipyrine and propyphenazone: Mass spectrometric and theoretical insights

ARTICLE *in* JOURNAL OF MASS SPECTROMETRY · JULY 2010

Impact Factor: 2.38 · DOI: 10.1002/jms.1763 · Source: PubMed

7 AUTHORS, INCLUDING:

Liulin Deng
Pacific Northwest National Laboratory
13 PUBLICATIONS **126** CITATIONS
SEE PROFILE

Huijun Guo
University of Science and Technology of Ch…
17 PUBLICATIONS **259** CITATIONS
SEE PROFILE

Yang Pan
University of Science and Technology of Ch…
44 PUBLICATIONS **304** CITATIONS
SEE PROFILE

Hao Yin
National High Magnetic Field Laboratory
13 PUBLICATIONS **116** CITATIONS
SEE PROFILE

Research Article

Journal of MASS SPECTROMETRY

Received: 6 February 2010 Accepted: 5 May 2010 Published online in Wiley Interscience: 25 May 2010

(www.interscience.com) DOI 10.1002/jms.1763

VUV photon-induced ionization/dissociation of antipyrine and propyphenazone: mass spectrometric and theoretical insights

Liulin Deng,[a] Lidong Zhang,[a] Huijun Guo,[a] Liangyuan Jia,[a] Yang Pan,[a] Hao Yin[b] and Fei Qi[a]*

Two analgesic and anti-inflammatory drugs, antipyrine and propyphenazone, were investigated with infrared laser desorption/tunable synchrotron vacuum ultraviolet (VUV) photoionization mass spectrometry (IR LD/VUV PIMS) and theoretical calculations. Mass spectra of the two drugs were measured at various photon energies. Fragment ions were gradually produced as photon energy increases. The structural assignment of the dominant fragment ions was supported by the results from a commercial electron impact time-of-flight mass spectrometer (EI-TOF MS). Primary fragmentation pathways were established from experimental observations combining with theoretical calculations. Methyl radical elimination is a common fragmentation pathway for two analytes. However, for propyphenazone cation, isopropyl group elimination to form antipyrine cation is another competitive pathway.

Supporting information may be found in the online version of this article.

Keywords: VUV photoionization mass spectrometry; laser desorption; antipyrine; propyphenazone; fragmentation pathway

Introduction

Antipyrine derivates (APDs) with broad chemical properties have been applied in many fields. In pharmacology, APDs have been widely used as an effective antitumor,[1] antimicrobial,[2–6] antiviral,[7] analgesic,[8] anti-inflammatory[9] and anticancer drugs.[10] In coordination chemistry, APDs were used as important ligands in synthesizing complexes with metal ions.[11] Moreover, APDs have been further investigated as a new type of nonlinear optoelectronic materials according to their promising optical characteristics.[12,13] Due to the profound potential applications of APDs, several protocols to synthesize new heterocycles derivates were reported.[2,14–16] Several APDs have been characterized with elemental analysis, FT-IR, FT-Raman, UV–vis spectroscopy and X-ray single crystal diffraction techniques combining with density functional theory calculations.[17] However, the investigation into gaseous ionization and dissociation mechanism of neutral APDs has scarcely been reported, which is complementary for understanding chemical properties of APDs.

Recently we developed infrared laser desorption (IR LD) combined with tunable vacuum ultraviolet (VUV) photoionization mass spectrometry (IR LD/VUV PIMS), which offers a unique advantage over conventional electron ionization (EI) methods in fragmentation study. IR LD/VUV PIMS can produce exclusive molecular ion without any fragments by choosing the VUV photon energy near ionization threshold. Furthermore, the fragmentation can be controlled by changing VUV photon energy.[18–22] In this study, we utilized IR LD/VUV PIMS to investigate the photoionization and photon-induced fragmentation of antipyrine and propyphenazone. The molecular ions were measured via near-threshold photoionization and a variety of fragment ions were observed with the photon energy increasing. The commercial EI (70 eV) time of flight (TOF) with high mass accuracy was utilized to confirm the structural formula of corresponding fragment ions. The major fragmentation pathways of these two drugs were proposed and discussed in detail, based on experimental measurements and theoretical calculations. Additionally, ionization energies (IEs) of antipyrine and propyphenazone were obtained by measurements of photoionization efficiency (PIE) spectra.

Experimental and Theoretical Methods

The experimental setup was reported in detail previously.[20–22] The equipment utilized a pulsed Nd:YAG laser (Surelite I-20, Continuum, USA) with 1064 nm output (10 Hz) as the laser desorption. The laser beam was focused on the substrate surface with a spot around 1.0 mm in diameter. In order to generate intact neutral molecules, laser power was controlled about 6 mJ/pulse in this study. Tunable VUV light beam from a synchrotron electron storage ring was perpendicular and overlapped with the desorption plume in the photoionization region. Neutral molecules were ionized at the cross-section between the VUV light and the dispersed plume, and produced ions were analyzed by a homemade reflection time-of-flight mass spectrometer (TOF MS). The pulsed voltage of 464 V with a frequency of 10 kHz applied

* *Correspondence to: Fei Qi, National Synchrotron Radiation Laboratory, University of Science and Technology of China, Hefei, Anhui 230029, P. R. China. E-mail: fqi@ustc.edu.cn*

a *National Synchrotron Radiation Laboratory, University of Science and Technology of China, Hefei, Anhui 230029, P. R. China*

b *Hefei National Laboratory for Physical Sciences at Microscale, University of Science and Technology of China, Hefei 230026, P. R. China*

Journal of MASS SPECTROMETRY

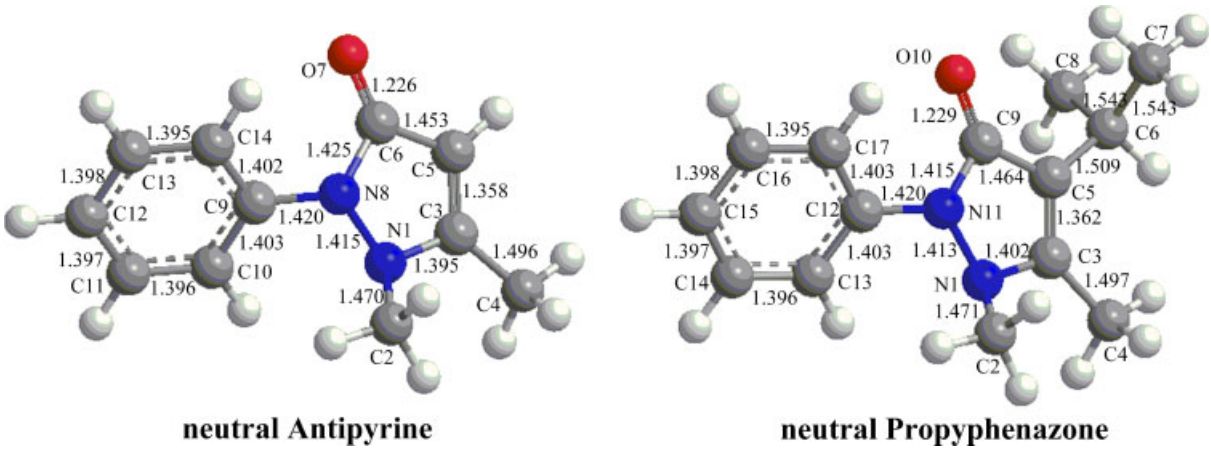

Figure 1. Optimized lowest energy structures for neutral antipyrine and propyphenazone (bond length in Å).

to a repeller plate was used to extract ions into the flight tube. The pressure of photoionization chamber was around 5.0×10^{-5} Pa. The sample was deposited in the stainless steel substrate without any matrix.

Synchrotron radiation from an undulator of the 800 MeV electron storage ring of National Synchrotron Radiation Laboratory (NSRL) was monochromatized with a 1 m Seya-Namioka monochromator equipped with a laminar grating (1500 grooves/mm, Horiba Jobin Yvon, France). This grating covered the photon energy from 7.8 to 24.0 eV. The monochromator was calibrated with known IEs of inert gases. The energy resolving power ($E/\Delta E$) was about 1000. A gas filter filled with neon or argon was used to eliminate higher order radiation. The average photon flux was measured to be around 1×10^{13} photons/s. A silicon photodiode (SXUV-100, International Radiation Detectors, Inc., USA) was used to monitor the photon flux for normalizing ion signals.

To confirm the structural assignments of fragment ions in proposing the fragmentation pathways, accurate mass measurements were performed with a gas chromatography (GC) TOF MS (Micromass, Manchester, UK) with 70 eV electron impact and trap current of 10 mA. The instrument was calibrated at a mass resolution of 8000 (FWHM) using heptacosafluorotributylamine as internal reference and the single point lock-mass was at *m/z* 218.9856. Sample analysis, exact mass measurements and elemental composition determination were performed automatically using the OpenLynx software (Micromass).

All the theoretical calculations were carried out using Gaussian 03 program.[23] The main decomposition pathways of antipyrine and propyphenazone cations were calculated using density functional theory employing the Becke-3-Lee-Yang-Parr (B3LYP) hybrid function and the 6-31+G(d,p) basis set.[24] The stationary points were identified with frequency calculations at the same level to verify that minima and transition state structures have zero and one imaginary frequencies, respectively. Zero-point energy (ZPE) corrections were also evaluated from the frequency calculations. The optimized lowest-energy structures for neutral antipyrine and propyphenazone were shown in Fig. 1. In the dissociation pathways of antipyrine and propyphenazone cations, the energies of corresponding neutral molecules were defined to be zero. The appearance energy (AE) of ionic fragment is defined as $E_{AE} = E_{max} - E_0$, in which E_{max} refers to the highest energy barrier involved in the formation pathway of corresponding ionic fragment and E_0 is the absolute energy of neutral precursor. In this work, the energies of the species involved in the dissociation of the analyte cations were electronic energies with ZPE correction, which are given in Table S3.

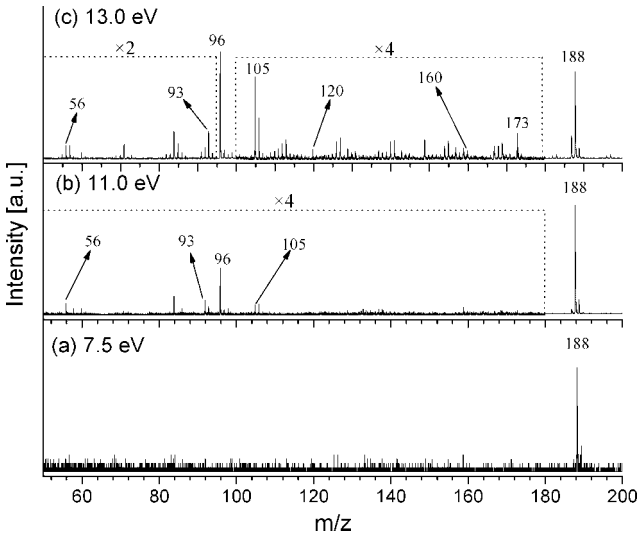

Figure 2. Photoionization mass spectra of antipyrine at photon energies of (a) 7.5 eV, (b) 11.0 eV, and (c) 13.0 eV.

Results and Discussion

VUV photoionization mass spectra

Photoionization mass spectra of antipyrine and propyphenazone measured at different photon energies are displayed in Figs. 2 and 3, the PIE spectra of two analytes are displayed in Fig. 4. Additionally, the EI mass spectra of two compounds are provided in the Supplementary Material.

Antipyrine

Figure 2 displays mass spectra of antipyrine at the photon energies of 7.5, 11.0 and 13.0 eV. Exclusive molecular ion $[M]^+$ (*m/z* 188) is observed at the photon energy of 7.5 eV. Fragment ions are yielded gradually as the photon energy increases. At the photon

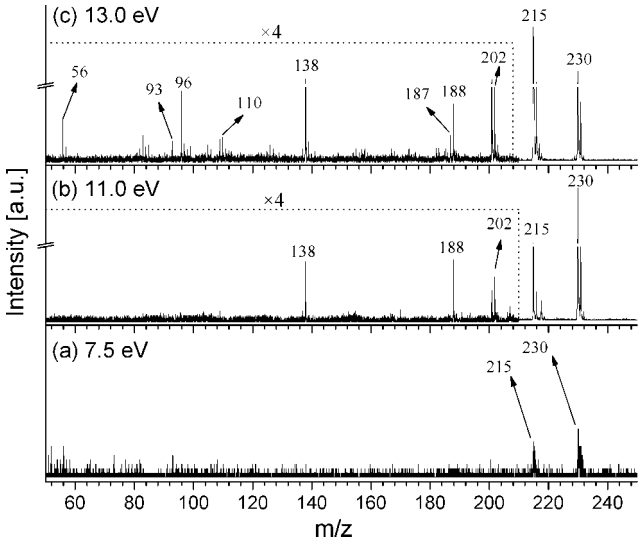

Figure 3. Photoionization mass spectra of propyphenazone at photon energies of (a) 7.5 eV, (b) 11.0 eV, and (c) 13.0 eV.

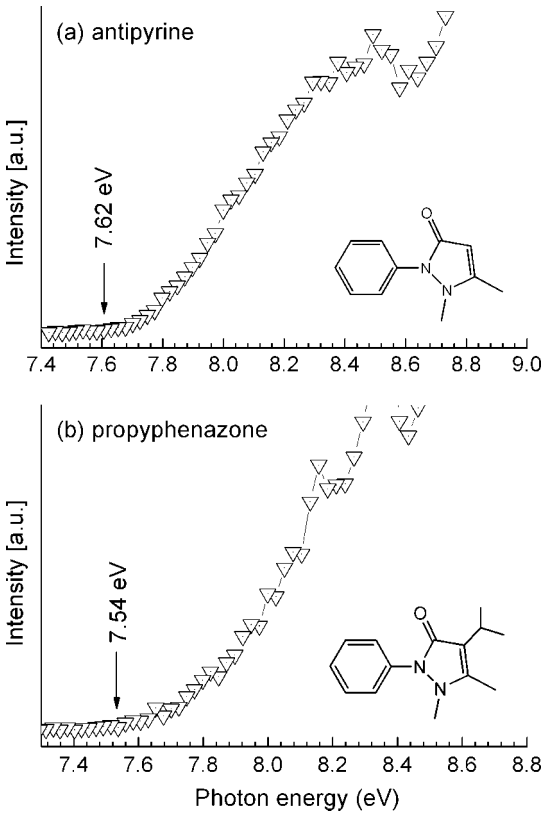

Figure 4. Photoionization efficiency spectra of (a) antipyrine and (b) propyphenazone.

energy of 11.0 eV, several ionic fragments *m/z* 105, 96, 93 and 56 are produced, besides the molecular ion. When the photon energy increases to 13.0 eV, more fragment ions *m/z* 173, 160 and 120 are detected. It is proposed that molecular ion directly eliminates C_4H_4O group to give *m/z* 120. Subsequently, *m/z* 120 loses CH_3 radical to form *m/z* 105. The *m/z* 96 and 93 are assigned to $[M\text{-}C_6H_6N]^+$ and $[M\text{-}C_5H_5NO]^+$, respectively. Also, CO elimination from the molecular ion forms *m/z* 160, which loses C_7H_6N group to produce *m/z* 56. The PIE spectrum of antipyrine is shown in Fig. 4a, which exhibits an ambiguous onset and extends toward lower photon energy. Some factors, for example hot band effect from laser heating and weak Frank-Condon factor, are responsible for the gradual onset near IE threshold. Attempts have been made to explain the thermal tail and step-like character in PIE spectra of molecules previously.[25]

Accurate elemental compositions of fragment ions yielded from antipyrine cation are confirmed by the OpenLynx software of commercial GCT TOF MS. From Fig. S1, several fragment ions at *m/z* 173.0730, 159.0908, 121.0776, 105.0548, 96.0451, 93.0577 and 56.0501 correspond to $[M\text{-}CH_3]^+$, $[M\text{-}CHO]^+$, $[M\text{-}C_4H_3O]^+$, $[M\text{-}C_5H_7O]^+$, $[M\text{-}C_6H_6N]^+$, $[M\text{-}C_5H_5NO]^+$ and $[M\text{-}C_8H_6NO]^+$, which are in good agreement with the outcomes of PI MS in this work (see Table S1).

Propyphenazone

Figure 3 shows photoionization mass spectra of propyphenazone at different photon energies. At the photon energy of 7.5 eV, molecular ion $[M]^+$ (*m/z* 230) is observed accompanied by a fragment ion *m/z* 215, which is attributed to $[M\text{-}CH_3]^+$. When the photon energy increases to 11.0 eV, *m/z* 202, 188 and 138 are produced, which are assigned to $[M\text{-}CO]^+$, $[M\text{-}C_3H_6]^+$ and $[M\text{-}C_6H_6N]^+$. More fragment ions at *m/z* 187, 110, 96, 93 and 56 are produced when the photon energy increases to 13.0 eV. The *m/z* 187 corresponds to the elimination of CO from $[M\text{-}CH_3]^+$ or loss of CH_3 radical from $[M\text{-}CO]^+$. The *m/z* 110 is formed by two formation pathways: (1) it is produced from the molecular ion by direct elimination of $C_7H_8N_2$ group and (2) the molecular ion loses C_6H_6N group to yield *m/z* 138, which then eliminates CO to produce *m/z* 110. Highly accurate EI mass spectrum of propyphenazone is shown in Fig. S2. Similar to the experimental results of PI MS, fragment ions such as *m/z* 215.1166, 202.1101, 187.1205, 138.0925, 96.0817 and 56.0498 are determined to be $[M\text{-}CH_3]^+$, $[M\text{-}CO]^+$, $[M\text{-}C_2H_3O]^+$, $[M\text{-}C_6H_6N]^+$, $[M\text{-}C_9H_{12}N]^+$ and $[M\text{-}C_{11}H_{12}NO]^+$ ions with OpenLynx software (see Table S2).

Fragmentation pathways

The fragmentation pathways of antipyrine and propyphenazone are discussed in detail with the help of theoretical calculations, as shown in Figs. 5–9. The detailed information on the geometries and energies (with ZPE correction) of the optimized reactants, transition states, intermediates and products involved in the dissociation of two analyte cations are shown in Figs. S3 and S4 and Table S3.

Antipyrine

There are two competitive fragmentation channels of antipyrine cation (RC1) to form the fragment ion *m/z* 173 (PC1-1, PC1-2) via direct elimination of the methyl radical located at N1 or C3, as shown in Fig. 5. The AEs of PC1-1 and PC1-2 are calculated to be 9.59 and 12.42 eV, respectively, which demonstrates that the fragmentation pathway to form PC1-1 is more feasible than that to form PC1-2.

One hydrogen atom on C2 is transferred to N8 to form intermediate INT1 via transition state TS1 overcoming an energy barrier of 2.78 eV. Then two competitive dissociation pathways are involved in the formation of PC2 (*m/z* 96) with loss of C_6H_6N group and PC4 (*m/z* 120) by eliminating C_4H_4O group. In the formation

Journal of MASS SPECTROMETRY

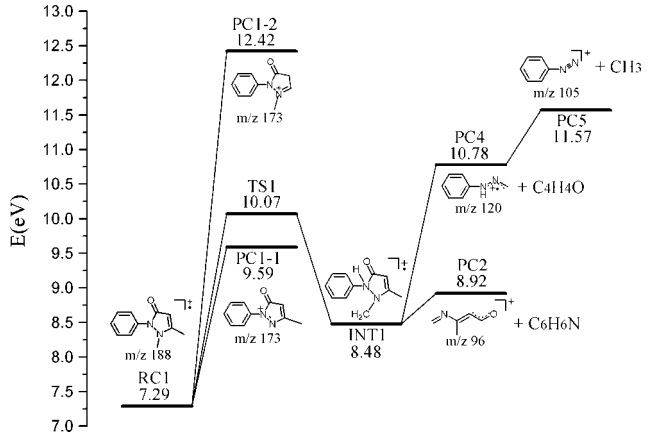

Figure 5. The dissociation pathways of the RC1 cation to produce fragment ions *m/z* 173, 96, 120 and 105. The relative energies E (with ZPE, eV) were calculated at the B3LYP/6-31+g(d,p) level. The energy of the neutral RC1 is defined to be zero.

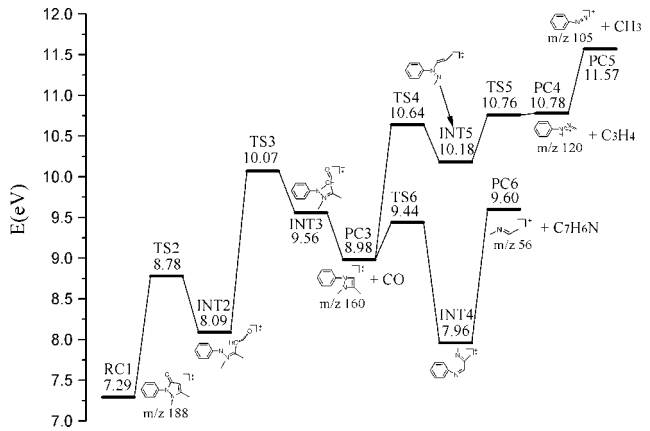

Figure 6. The formation pathway of fragment ions *m/z* 160, 120, 105 and 56 from the RC1. The relative energies E (with ZPE, eV) were calculated at the B3LYP/6-31+g(d,p) level. The energy of the neutral RC1 is defined to be zero.

pathway of PC2, theoretical results suggest that INT1 suffers from N1–N8 and C6–N8 bond cleavages with the dissociation energy of 0.44 eV. In the formation pathway of PC4, INT1 eliminates C_4H_4O group via N8–C6 and N1–C3 bond cleavages, and the corresponding dissociation energy is 2.30 eV. Further loss of the methyl radical from PC4 yields PC5 (*m/z* 105) with a dissociation energy of 0.79 eV.

The other pathways to form PC4 and PC5 are shown in Fig. 6. First, pyrazole ring rearranges to form INT3 with four-member heterocycle via TS2 and TS3. The energy barriers of these two steps are calculated to be 1.49 and 1.98 eV, respectively. Then INT3 eliminates CO to yield PC3 (*m/z* 160). The further isomerization of PC3 generates INT5 via ring-opening transition state TS4. PC4 and PC5 can be produced through the sequent bond cleavage of INT5. The other competitive dissociation pathway of PC3 is involved in the formation of PC6 (*m/z* 56), PC3 undergoes N1–N8 bond cleavage with a barrier of 0.46 eV at TS6, which generates INT4. Subsequently, C3–C5 bond ruptures to yield PC6 by loss of C_7H_6N group.

According to the calculations, the AEs of PC1-1, PC2, PC3, PC6, PC4 and PC5 are gradually increased, which are in good agreement

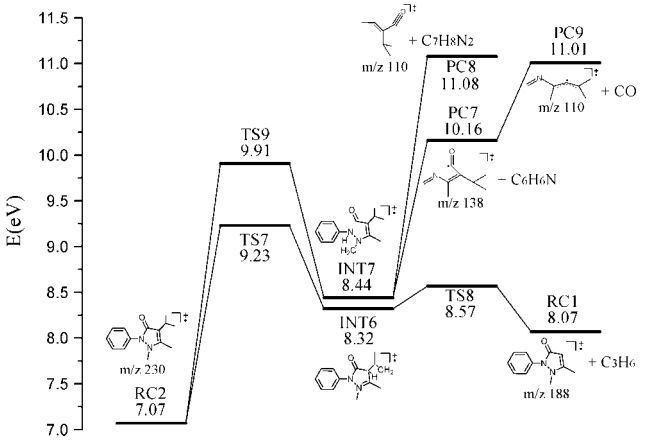

Figure 7. The dissociation pathways of the RC2 cation to produce fragment ions *m/z* 188, 138 and 110. The relative energies E (with ZPE, eV) were calculated at the B3LYP/6-31+g(d,p) level. The energy of the neutral RC2 is defined to be zero.

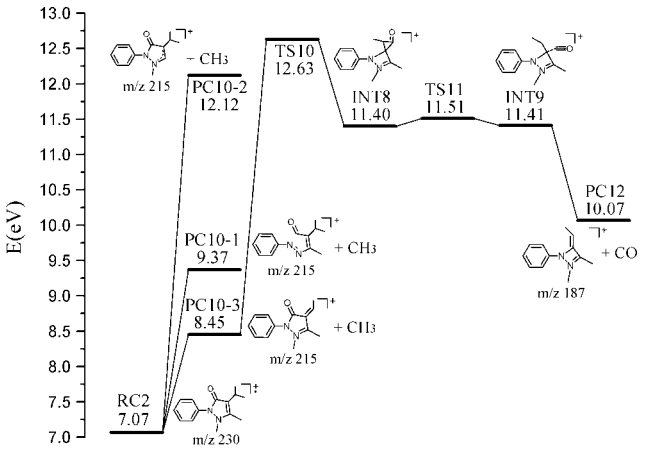

Figure 8. The dissociation pathways of the RC2 cation to produce fragment ions *m/z* 215 and 187. The relative energies E (with ZPE, eV) were calculated at the B3LYP/6-31+g(d,p) level. The energy of the neutral RC2 is defined to be zero.

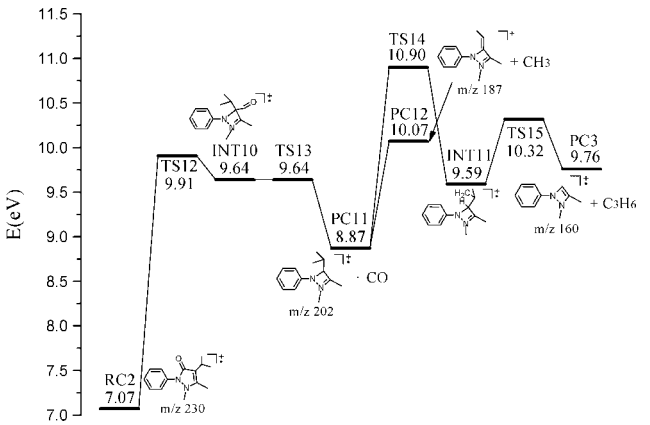

Figure 9. The formation pathway of fragment ions *m/z* 202, 187 and 160 from the RC2. The relative energies E (with ZPE, eV) were calculated at the B3LYP/6-31+g(d,p) level. The energy of the neutral RC2 is defined to be zero.

with the experimental observations. Fragment ion *m/z* 96 (PC2) is the stable one, which is 8.92 eV relative to neutral antipyrine. The experimental measurement confirms that *m/z* 96 has the highest ion intensity (Fig. 2b and c).

Propyphenazone

Figure 7 shows that propyphenazone cation (RC2) undergoes hydrogen atom shift to C5 from C8 to yield INT6 via TS7, the barrier of this step is calculated to be 2.16 eV. The antipyrine cation RC1 (*m/z* 188) is yielded by losing C_3H_6 group via TS8 with a barrier of 0.25 eV. The C9–N11 bond fission accompanied by intramolecular hydrogen transfer from C2 to N11 leads to form INT7 via TS9 with a barrier of 2.84 eV. From INT7, two competitive fragmentation pathways are involved in the production of *m/z* 110 (PC8, PC9): first, the N1–N11 bond undergoes elongation and fission followed by the elimination of C_6H_6N group to generate PC7 (*m/z* 138), which subsequently eliminates CO to produce PC9; second, INT7 directly eliminates $C_7H_8N_2$ group via N1–C3 bond fission with a dissociation energy of 2.64 eV to produce PC8, which is an isomer of PC9.

There are three competitive methyl elimination pathways to produce *m/z* 215 (PC10-1, PC10-2 and PC10-3), as shown in Fig. 8. PC10-1 and PC10-2 are yielded by directly losing the methyl radical from the pyrazole ring with N1–C2 and C3–C4 bond fissions, respectively. The calculated AEs of these two fragment ions are 9.37 and 12.12 eV at B3LYP/6-31+G(d,p) level, respectively. Besides, C6–C7 or C6–C8 bond cleavage to eliminate methyl radical from the isopropyl group can yield PC10-3. Moreover, the AE of PC10-3 is calculated to be 8.45 eV, which is the lowest one among the three methyl elimination pathways, and thus it is deemed that PC10-3 contributes predominantly for *m/z* 215. The formation of PC12 (*m/z* 187) from PC10-3 is proposed via two transition states and two intermediates. Initially, N11–C9 bond cleavage and N11–C5 bond formation lead to the formation of INT8 via TS10. The calculated barrier of the process is 4.18 eV. Subsequently, INT9 is formed via INT8 rearrangement with TS11 (0.11 eV relative to INT8), PC12 is finally produced by elimination of CO.

From Fig. 9, RC2 undergoes pyrazole ring rearrangement to form INT10 via TS12 with an energy barrier of 2.84 eV. Then, INT10 loses CO to produce PC11 (*m/z* 202) via TS13. PC11 directly eliminates the methyl radical from the isopropyl group to yield PC12. Besides, the intramolecular hydrogen transfer in PC11 leads to form INT11 via TS14, and PC3 (*m/z* 160) is finally yielded with the C5–C6 bond cleavage to lose propylene moiety. The energy barriers of these two steps are 2.03 and 0.73 eV, respectively. Moreover, the further dissociation pathways of PC3 have been discussed in Section 2.1.

Above all, PC10-3, RC1, PC11 and PC7 have low AEs, which are in good agreement with the experimental results that *m/z* 215, 188, 202 and 138 appear at low photon energy and with high intensities. Furthermore, theoretical calculations show that RC1 (*m/z* 188) is stable, which is 8.07 eV relative to neutral propyphenazone. This is consistent with the experimental observation (Fig. 3b and c).

In summary, the low-energy methyl elimination pathways of two drugs are different. The C–C bond cleavage at the isopropyl group is predominant for propyphenazone, however, the C–N bond cleavage from pyrazole ring to lose methyl radical is more feasible for antipyrine. CO elimination of both drugs has analogous dissociation channels to form products with four-member heterocycle via rearrangement of pyrazole ring. Other dissociation pathways of antipyrine and propyphenazone undergo pyrazole ring-opening dissociation followed by intramolecular hydrogen transfer.

Conclusions

Two drugs, antipyrine and propyphenazone, have been studied using IR LD/VUV PIMS and theoretical calculations. The molecular ions are produced via near-threshold photoionization, and fragment ions are observed at higher photon energy. The structural assignments of the fragment ions are supported by accurate EI-TOF MS measurements. Additionally, The IEs of these two drugs have been measured to be 7.62 and 7.54 $\pm$ 0.1 eV, respectively.

Methyl, CO eliminations and pyrazole ring-opening dissociation are the predominant fragmentation pathways of these two analytes. The ion $[M\text{-}CH_3]^+$ is the primary fragments from both analytes, however, they have different predominant methyl elimination pathways due to the isopropyl substitution of propyphenazone. Furthermore, they have the analogous fragmentation channels to form CO elimination products by pyrazole ring rearrangement and other products by pyrazole ring-opening dissociation. Propyphenazone cation can directly eliminate the isopropyl radical to form antipyrine cation.

Acknowledgements

This work has been supported by grants from Chinese Academy of Sciences (YZ200764) and the Natural Science Foundation of China (10705026, 10805047 and 50925623).

Supporting information

Supporting information may be found in the online version of this article.

References

[1] E. Radzikowska, K. Onish, E. Chojak. Prospective assessment of cancer incidence and antipyrine metabolism. *Eur. J. Cancer* **1995**, *31A*, 1077.
[2] S. Bondock, R. Rabie, H. A. Etman, A. A. Fadda. Synthesis and antimicrobial activity of some new heterocycles incorporating antipyrine moiety. *Eur. J. Med. Chem.* **2008**, *43*, 2122.
[3] S. Cunha, S. M. Oliveira, M. T. Rodrigues, R. M. Bastos, J. Ferrari, C. M. A. de Oliveira, L. Kato, H. B. Napolitano, I. Vencato, C. Lariucci. Structural studies of 4-aminoantipyrine derivatives. *J. Mol. Struct.* **2005**, *752*, 32.
[4] A. P. Mishra. Physicochemical and antimicrobial studies on nickel(II) and copper(II) Schiff base complexes derived from 2-furfuraldehyde. *J. Indian Chem. Soc.* **1999**, *76*, 35.
[5] N. Raman, A. Kulandaisamy, K. Jeyasubramanian. Synthesis, spectral, redox, and antimicrobial activity of Schiff base transition metal(II) complexes derived from 4-aminoantipyrine and benzil. *Synth. React. Inorg. Met.-Org. Chem.* **2002**, *32*, 1583.
[6] N. Raman, A. Kulandaisamy, K. Jeyasubramanian. Synthesis, structural characterization, redox, and antibacterial studies of 12-membered tetraaza macrocyclic Cu(II), Ni(II), Co(II), Zn(II), and VO(IV) complexes derived from 1,2-(diimino-4 '-antipyrinyl)-1,2-diphenylethane and o-phenylenediamine. *Synth. React. Inorg. Met.-Org. Chem.* **2004**, *34*, 17.
[7] M. Mahmoud, R. Abdel-Kader, M. Hassanein, S. Saleh, S. Botros. Antipyrine clearance in comparison to conventional liver function tests in hepatitis C virus patients. *Eur. J. Pharmacol.* **2007**, *569*, 222.
[8] S. M. Sondhi, V. K. Sharma, R. P. Verma, N. Singhal, R. Shukla, R. Raghubir, M. P. Dubey. Synthesis, anti-inflammatory and analgesic activity evaluation of some mercapto pyrimidine and pyrimidobenzimidazole derivatives. *Synthesis-Stuttgart* **1999**, 878.

[9] M. M. F. Ismail, Y. A. Ammar, H. S. A. El-Zahaby, S. I. Eisa, S. E. S. Barakat. Synthesis of novel 1-pyrazolylpyridin-2-ones as potential anti-inflammatory and analgesic agents. *Arch. Pharm. Chem. Life Sci.* **2007**, *340*, 476.
[10] S. M. Sondhi, N. Singhal, R. P. Verma, S. K. Arora, S. G. Dastidar. Synthesis of hemin and porphyrin derivatives and their evaluation for anticancer activity. *Indian J. Chem. Sect. B-Org. Chem. Incl. Med. Chem.* **2001**, *40*, 113.
[11] M. Gaber, A. M. Hassanein, A. A. Lotfalla. Synthesis and characterization of Co(II), Ni(II) and Cu(II) complexes involving hydroxy antipyrine azodyes. *J. Mol. Struct.* **2007**, *875*, 322.
[12] M. S. Collado, V. E. Mantovani, H. C. Goicoechea, A. C. Olivieri. Simultaneous spectrophotometric-multivariate calibration determination of several components of ophthalmic solutions: phenylephrine, chloramphenicol, antipyrine, methylparaben and thimerosal. *Talanta* **2000**, *52*, 909.
[13] S. A. J. Coolen, T. Ligor, M. van Lieshout, F. A. Huf. Determination of phenolic derivatives of antipyrine in plasma with solid-phase extraction and high-performance liquid chromatography-atmospheric-pressure chemical ionization mass spectrometry. *J. Chromatogr. B* **1999**, *732*, 103.
[14] E. S. H. Ei Ashry, L. F. Awad, E. I. Ibrahim, O. K. Bdeewy. Synthesis of antipyrine derivatives derived from dimedone. *Chin. J. Chem.* **2007**, *25*, 570.
[15] A. Gürsoy, S. Demirayak, G. Çapan, K. Erol, K. Vural. Synthesis and preliminary evaluation of new 5-pyrazolinone derivatives as analgesic agents. *Eur. J. Med. Chem.* **2000**, *35*, 359.
[16] G. L. Turan-Zitouni, M. Sivaci, F. S. Kilic, K. Erol. Synthesis of some triazolyl-antipyrine derivatives and investigation of analgesic activity. *Eur. J. Med. Chem.* **2001**, *36*, 685.
[17] Y. X. Sun, Q. L. Hao, W. X. Wei, Z. X. Yu, L. D. Lu, X. Wang, Y. S. Wang. Experimental and density functional studies on 4-(2, 3-dichlorobenzylideneamino) antipyrine and 4-(2, 5-dichlorobenzylideneamino)antipyrine. *J. Mol. Struct.* **2009**, *929*, 10.
[18] Y. Pan, H. Yin, T. C. Zhang, H. J. Guo, L. S. Sheng, F. Qi. The characterization of selected drugs with infrared laser desorption/tunable synchrotron vacuum ultraviolet photoionization mass spectrometry. *Rapid Commun. Mass Spectrom.* **2008**, *22*, 2515.
[19] Y. Pan, L. D. Zhang, H. J. Guo, F. Qi. Dissociative photoionization mechanism of 1,8-dihydroxyanthraquinone: an experimental and theoretical study. *J. Phys. Chem. A* **2008**, *112*, 10977.
[20] Y. Pan, L. D. Zhang, T. C. Zhang, H. J. Guo, X. Hong, F. Qi. Photoionization studies on various quinones by an infrared laser desorption/tunable VUV photoionization TOF mass spectrometry. *J. Mass Spectrom.* **2008**, *43*, 1701.
[21] Y. Pan, T. C. Zhang, X. Hong, Y. W. Zhang, L. S. Sheng, F. Qi. Fragment-controllable mass spectrometric analysis of organic compounds with an infrared laser desorption/tunable vacuum ultraviolet photoionization technique. *Rapid Commun. Mass Spectrom.* **2008**, *22*, 1619.
[22] Y. Pan, L. D. Zhang, H. J. Guo, L. L. Deng, F. Qi. Photoionisation and photodissociation studies of nonvolatile organic molecules by synchrotron VUV photoionisation mass spectrometry and theoretical calculations. *Int. Rev. Phys. Chem.* **2010**, *29*, 369.
[23] M. J. Frisch, G. W. Trucks, H. B. Schlegel, *et al*. *Gaussian 03, Revision C. 02*, Gaussian, Inc.: Wallingford, CT., **2004**.
[24] A. D. Becke. Density-functional thermochemistry. The pole of exact exchange. *J. Chem. Phys.* **1993**, *98*, 5648.
[25] H. Tsunoyama, F. Misaizu, K. Ohno. Photoionization efficiency curve measurements of alkali metal atom-methyl propiolate clusters: observation of intracluster cyclotrimerization products. *J. Phys. Chem. A* **2004**, *108*, 5.

